

Cues for vertical localization in the upper median plane: Integrating directional band theory and parametric notch-peak model

Kazuhiro Iida^{1,a)} and Fuka Nakamura²

¹*Spatial Hearing Laboratory, Faculty of Advanced Engineering, Chiba Institute of Technology, Narashino, Chiba, 275-0016 Japan*

²*Spatial Hearing Laboratory, Graduate School of Engineering, Chiba Institute of Technology, Narashino, Chiba, 275-0016 Japan*

ABSTRACT:

A number of studies have examined cues for the perception of the vertical angle of a sound image. Sound localization tests using narrow-band signals revealed that there exist directional bands that were perceived in specific directions (front, above, and rear), regardless of the direction of the actual sound source. On the other hand, sound localization tests using wideband signals revealed that spectral notches and peaks above 5 kHz in the head-related transfer function (HRTF) contribute to vertical angle perception. Based on this finding, a parametric notch-peak (PNP) HRTF model, which is reconstructed using the minimum number of notches and peaks required for vertical angle perception, has been proposed. Thus, the directional band theory, which claims that the presence of specific frequency components is important, and the PNP model, which suggests the importance of the absence of specific frequency components (notches), appear to be contradictory. In the present study, we first focus on the front, above, and rear directions and attempt to integrate the PNP model and the directional band theory. Then, expanding the scope to the entire upper median plane, a hypothesis regarding the cues for vertical angle perception and the extended PNP model is proposed. © 2025 Acoustical Society of America. <https://doi.org/10.1121/10.0041787>

(Received 1 April 2025; revised 23 October 2025; accepted 17 November 2025; published online 4 December 2025)

[Editor: Jonas Braasch]

Pages: 4406–4417

I. INTRODUCTION

Around 1900, it was found that the interaural time difference and the interaural level difference are cues for the perception of the lateral angle of a sound image (Lord Rayleigh, 1877, 1907). Afterward, around 1960, the quantitative relationships between these interaural differences and the lateral angle of a sound image were reported (Sayers, 1964; Toole and Sayers, 1965). After the 1970s, a number of studies examined cues for the perception of the vertical angle of a sound image. Consequently, it was found that cues exist in the amplitude spectrum of the head-related transfer function (HRTF). These are referred to as spectral cues. Moreover, studies to find the specific important part of the amplitude spectrum that acts as a spectral cue have been performed.

Blauert (1969/70) conducted sound localization tests, in which narrow-band signals (1/3-octave-band noise) were presented randomly from the front, above, and rear in the median plane in an anechoic chamber and reported that there were bands in which sound images were perceived in specific directions (front, above, and rear), regardless of the direction of the sound source. These bands are referred to as directional bands.

On the other hand, sound localization tests using wideband signals revealed that spectral notches and peaks above

5 kHz contribute to the perception of the vertical angle of a sound image (Hebrank and Wright, 1974; Butler and Belendiuk, 1977; Mehrgardt and Mellert, 1977; Musicant and Butler, 1984). The frequency of notches shifts higher as the sound source moves from the front of the subject to above the subject (Butler and Belendiuk, 1977; Shaw and Teranishi, 1968), and the difference in notch frequency due to the vertical angle has been reported to be detectable by the listener (Moore *et al.*, 1989). Therefore, this vertical angle dependency of the notch frequency is thought to be one of the important cues for vertical localization. Based on these findings, the parametric notch-peak HRTF model (hereinafter referred to as the PNP model), recomposed of all or some of the spectral notches and peaks extracted from a listener's own HRTF, was proposed (Iida *et al.*, 2007).

Thus, the directional band theory, which claims that the presence of specific frequency components is important for the perception of vertical angle for narrow-band signals, and the PNP model, which claims the importance of the absence of specific frequency components (notches) for the perception of vertical angle for wideband signals, appear to be contradictory. This apparent contradiction raises fundamental questions regarding the mechanisms underlying vertical sound localization, which this study aims to resolve through an integrative model.

In the present study, we first focus on the three directions in the median plane—front, above, and rear—and discuss the results of previous research on the PNP model and

^{a)}Email: kazuhiro.iida@it-chiba.ac.jp

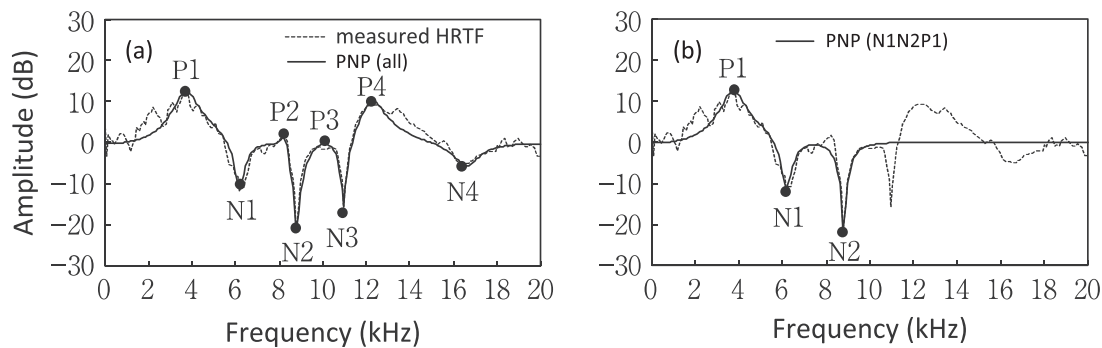


FIG. 1. Examples of PNP HRTF models: (a) measured HRTF (dotted line) and corresponding PNP model (solid line) with all notches and peaks; (b) PNP model reconstructed using only N1, N2, and P1.

the directional band theory together with recent analytical results, attempting to integrate these two findings. We then expand the scope of the sound source direction to the entire upper median plane and propose a hypothesis regarding the cues for the perception of vertical angle. Furthermore, we extend the PNP model based on this hypothesis.

II. PARAMETRIC NOTCH-PEAK HRTF MODEL AND DIRECTIONAL BAND THEORY FOR VERTICAL ANGLE PERCEPTION

We provide a detailed explanation of the PNP model and the directional band theory, which have been proposed as cues for vertical angle perception.

A. Parametric notch-peak HRTF model

Iida *et al.* (2007) proposed a PNP model recomposed of the spectral notches and peaks extracted from a listener's measured HRTF, regarding the peak around 4 kHz, which is independent of the vertical angle of the sound source (Shaw and Teranishi, 1968), as the lower-frequency limit. The notches and peaks are labeled in order of frequency (e.g., P1, N1, P2, N2, and so on). The notches and peaks are expressed parametrically in terms of center frequency, level, and Q-factor. Figure 1 shows examples of PNP models. The dotted line in Fig. 1(a) shows the measured HRTF for the front direction of a subject. This HRTF was decomposed into four notches and four peaks, and the HRTF reconstructed using all of them with the IIR filters is the PNP model (all) shown by the solid line. Sound localization tests were conducted using PNP models recomposed of various combinations of notches and peaks for seven target vertical angles (30° intervals) in the upper median plane. The stimuli in which the PNP model was convolved with wideband white noise were presented using free air equivalent coupling to the ear (FEC) headphones (Møller, 1992). The results showed that the minimum configuration of notches and peaks that could provide approximately the same sound localization accuracy to the measured HRTFs in all seven directions was two lowest-frequency notches (N1, N2) and one peak (P1) [Fig. 1(b)].

Subsequent sound localization tests revealed that P2 was necessary for some listeners for the above (zenith)

direction. As such, P2 was added to the minimum configuration for the PNP model for the above (Iida and Ishii, 2018) direction. Furthermore, recent research has found that a peak around 1 kHz contributes to the perception of a clear, unblurred sound image for the rear direction (Nakamura and Iida, 2025), and so P0, which reflects the peak around 1 kHz, was added to the rear PNP model. Table I shows the minimum configuration of the PNP model for seven directions in the upper median plane.

B. Directional band theory

Next, we provide a detailed explanation of the directional band theory. Blauert (1969/70) performed sound localization tests, in which 1/3-octave-band noise was presented randomly from loudspeakers placed in the front, above, and rear directions in the median plane in an anechoic chamber.

Subjects were asked to choose one of three areas to indicate the direction of the sound image they perceived: front, above, or rear. The results revealed that there were bands for which sound images were perceived in specific directions (front, above, or rear) regardless of the direction of the sound source. The center frequencies of the directional bands for the front are 315, 400, and 500 Hz and 3.15, 4, and 5 kHz, for above 8 kHz, and for the rear are 0.8, 1, 1.25, 1.6, 10, and 12.5 kHz. Thus, the frequency ranges for the front directional bands are 280–560 Hz and 2.8–5.6 kHz, the frequency range for the above directional band is 7.1–9.0 kHz, and the frequency ranges for the rear directional bands are 710 Hz–1.8 kHz and 9.0–14.0 kHz. These frequency ranges are the upper and lower cutoff frequencies of the five center frequency groups of the directional bands (315–500 Hz, 3.15–5 kHz, 8 kHz, 0.8–1.6 kHz, and 10–12.5 kHz).

TABLE I. Minimum components of the PNP model in the upper median plane.

Target vertical angle (deg.)	N1	N2	P1	P2	P0
0, 30, 60, 120, 150	x	x	x		
90	x	x	x	x	
180	x	x	x		x

Later, it was reported that directional bands were observed not only in 1/3-octave-band noise, but also in 1/6-, 1/12-, and 1/24-octave-band noise, and pure tones (Itoh *et al.*, 2007; Iida, 2019b).

Conversely, when stimuli were combined with consecutive bands (1.12–3.15, 4–4.5, and 6.3–9 kHz), in each of which the directional band of a 1/6-octave-band was observed in the same perceived direction—rear, front, and above, respectively—the directional band was also observed in the same direction as each of the 1/6-octave-bands (Iida, 2019b).

Furthermore, whether the directional bands also contribute to the perception of vertical angle for wideband signals was investigated. Wide-band white noise was convolved with one of the 1/3-octave-band boost filters with a center frequency of 1.25, 4, or 8 kHz (Table II), which represent the directional bands for the rear, front, and above directions, respectively, and presented to subjects in random order from loudspeakers placed in the front, above, and rear directions in an anechoic chamber (Iida, 2019b).

As a result, regardless of the center frequency and boosted level, responses were distributed in the direction of the loudspeakers. In other words, for wideband signals, boosting of the directional band did not affect the perception of vertical angle. However, for the boosted level of 18 dB or more, the sound image is sometimes separated into two. When the sound image was separated, the sound image for the non-boosted band was perceived in the direction of the loudspeakers, and the sound image for the boosted band was perceived in the direction of the directional bands. These results indicate that for wideband signals, the directional bands do not contribute, or do not contribute sufficiently, as a cue for perception of vertical angle.

III. INTEGRATION OF DIRECTIONAL BAND THEORY AND PARAMETRIC NOTCH-PEAK HRTF MODEL

Vertical localization for narrow-band signals, which can be explained by the directional bands, and vertical localization for wideband signals, which can be explained by the PNP model, are both highly reproducible auditory phenomena. Therefore, there must be a mechanism that can explain both without contradiction. In this section, we focus on the front, above, and rear directions in the median plane. We discuss previous research results and recent analytical results on the PNP model and the directional band theory, and then attempt to integrate the PNP model and the directional band theory.

A. Comparison of frequencies of notches and peaks and directional bands

First, we discuss the relationship between the vertical angle of a sound source in the median plane and the

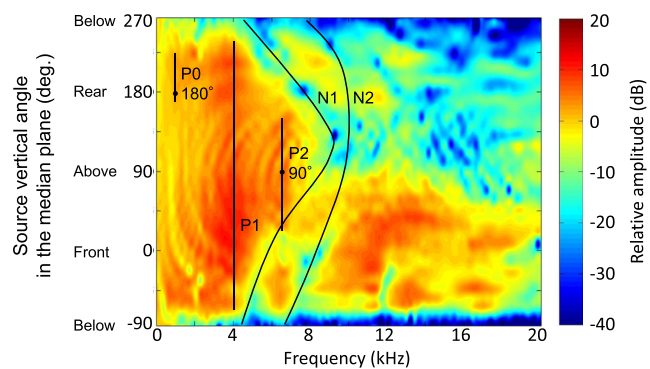


FIG. 2. Relative amplitude of the HRTFs for a representative subject in the median plane. Solid lines indicate N1, N2, P1, P2, and P0.

frequencies of notches and peaks. Figure 2 shows the relative amplitude of the HRTFs for a representative subject in the median plane. The red area indicates a high HRTF amplitude, and the blue area indicates a low HRTF amplitude. The notches and peaks are drawn as solid lines.

The N1 and N2 frequencies change continuously depending on the vertical angle of the sound source across the entire median plane. This suggests that the vertical angle dependence of the N1 and N2 frequencies acts as a cue for the perception of vertical angle. From a perceptual standpoint, such spectral notches may provide fine spatial resolution by reducing ambiguity among nearby vertical angles, working in a complementary manner with spectral peaks.

A closer examination reveals that both N1 and N2 frequencies increase with vertical angle up to 120°, and then begin to decrease beyond this point. Notably, N1 decreases more steeply than N2 as the angle approaches 270°. Therefore, the vertical angle of a sound source cannot be uniquely determined using either N1 frequency or N2 frequency alone. This explains why two notches are necessary for median plane localization. On the other hand, the frequencies of P1, P2, and P0 are almost independent of the sound source direction and are not considered to be cues for identifying the vertical angle of a sound source.

We then compare the frequencies of the peaks with those of the directional bands. Table III shows the median values of the P1, P2, and P0 frequencies for 118 ears. The frequency ranges of the Blauert (1969/70) directional bands for the front, above, and rear directions are shown in Table IV. These frequency ranges are the upper and lower cutoff frequencies of the five center frequency groups of the directional bands described in Sec. II B (315–500 Hz, 3.15–5 kHz, 8 kHz, 0.8–1.6 kHz, and 10–12.5 kHz). These tables suggest that the frequency of P1 coincides with that of one of the directional bands for front, the frequency of P2

TABLE III. Median values of the P1, P2, and P0 frequencies for 118 ears (kHz).

P1	P2	P0
4.0	8.3	1.0

TABLE II. Specifications of 1/3-octave-band boost filters.

Center frequency (kHz)	Band width (oct.)	Boosted level (dB)
1.25, 4, 8	1/3	6, 12, 18, 24, 30

TABLE IV. Frequency ranges of Blauert's directional bands for the front, above, and rear directions (kHz).

Front	Above	Rear
0.3–0.6, 2.8–5.6	7.1–9.0	0.7–1.8, 9.0–14.0

coincides with that of the directional band for above, and the frequency of P0 coincides with that of one of the directional bands for rear.

B. Hypothesis 1: Integration of parametric notch-peak HRTF model and directional band theory

Based on the findings above, Hypothesis 1 is derived as follows: the PNP model comprises notches and peaks, with the peak frequencies corresponding to those of the directional bands for the front, above, and rear directions.

IV. CUES FOR VERTICAL ANGLE PERCEPTION IN THE ENTIRE UPPER MEDIAN PLANE

In Sec. III, we discussed the integration of the PNP model and the directional band theory, focusing on three specific directions in the median plane: front, above, and rear. In this section, we extend the analysis to the entire upper median plane to investigate cues for vertical angle perception. Based on the findings from the analysis, we then propose Hypothesis 2.

A. Directional bands in the upper median plane

Itoh *et al.* (2007) conducted sound localization tests similar to those of Blauert, using 1/3- and 1/6-octave-band noise with center frequencies ranging from 0.8 to 12.5 kHz. Whereas Blauert (1969/70) asked subjects to select one of three directional categories (front, above, or rear), Itoh *et al.* more precisely obtained the perceived vertical angles by employing a mapping method.

Using the original 1/3-octave-band dataset from Itoh *et al.* (2007), we reanalyzed the subjects' vertical angle responses to examine whether directional bands appear not only at the front, above, and rear, but also continuously throughout the upper median plane. The reason why only the 1/3-octave-band data were used is to reanalyze the experimental data in the same way as Blauert's experiment and analysis. However, because their experiment included subjects with low localization accuracy for wideband white noise in the upper median plane, we limited our analysis to four subjects with high localization accuracy.

Following Blauert's method, Itoh *et al.* determined directional bands for the front, above, and rear directions using the following procedure. First, each subject's responses were classified into one of three directional categories based on the responded vertical angle: front (-45° to 45°), above (45° to 135°), and rear (135° to 225°). Second, a frequency band was considered a directional band if the number of responses in one category significantly exceeded

the combined number in the other two ($p < 0.05$), as determined by a binomial test.

However, with this method, for a given response distribution, increasing the number of directional categories reduces the angular range assigned to each category, thereby making it more difficult to determine whether a directional band is present. To address this limitation, the present study did not use predefined angular categories. Instead, we identified the range of vertical angles in which responses were most concentrated and determined whether this range constitutes a directional band. As a result, the representative vertical angles for each directional band are not necessarily limited to canonical angles such as 0° , 30° , 60° , 90° , 120° , 150° , or 180° .

The specific method used for directional band analysis in the present study is as follows. In the experiment by Itoh *et al.*, each stimulus was presented 10 times from each of the three directions—front, above, and rear—resulting in a total of 30 responses per stimulus for each subject. According to the binomial test, a bias in the response distribution is considered statistically significant at the 5% level when more than 20 out of 30 responses fall into the same category. Therefore, for each stimulus, the 30 responses were sorted in ascending order by vertical angle, and all possible groups of 20 consecutive responses were extracted. This yielded 11 groups in total: responses 1–20, 2–21, ..., 11–30. The vertical angle range of each group was calculated, and the smallest range was taken as the most concentrated cluster of responses. Following Blauert and Itoh *et al.*, who defined vertical angles of $0^\circ \pm 45^\circ$ as front, $90^\circ \pm 45^\circ$ as above, and $180^\circ \pm 45^\circ$ as rear, we considered a group to constitute a directional band if the minimum response range was within 90° . The median value of the 20 responses in that group was then adopted as the representative vertical angle for the directional band.

The results of the analysis are presented in Fig. 3. Responded vertical angles are depicted as circles, with the radius of each circle proportional to the relative number of responses. Vertical bars indicate the range of vertical angles that could be considered to be directional bands, and the "x" mark on each bar represents the median of those responses. For comparison, the directional bands for front, above, and rear as identified by Itoh *et al.* are shown at the top of the figure.

For subject 1, the response vertical angles increased from 0° to 178° as the center frequency of the stimuli increased from 0.8 to 12.5 kHz. However, the responses were distributed over a wide range of vertical angles at 0.8 and 1.6 kHz and between 6.3 and 10 kHz. Directional bands were observed at all center frequencies except 8 and 10 kHz. The median vertical angles that could be considered to be directional bands increased from 7° to 168° as the center frequency increased from 0.8 to 12.5 kHz, excluding 1.6 kHz.

The front, above, and rear directional bands analyzed by Itoh *et al.* were at 0.8–1.25 and 2.5 kHz for the front, 5 and 6.3 kHz for the above, and 12.5 kHz for the rear. At these frequencies, directional bands were observed in the

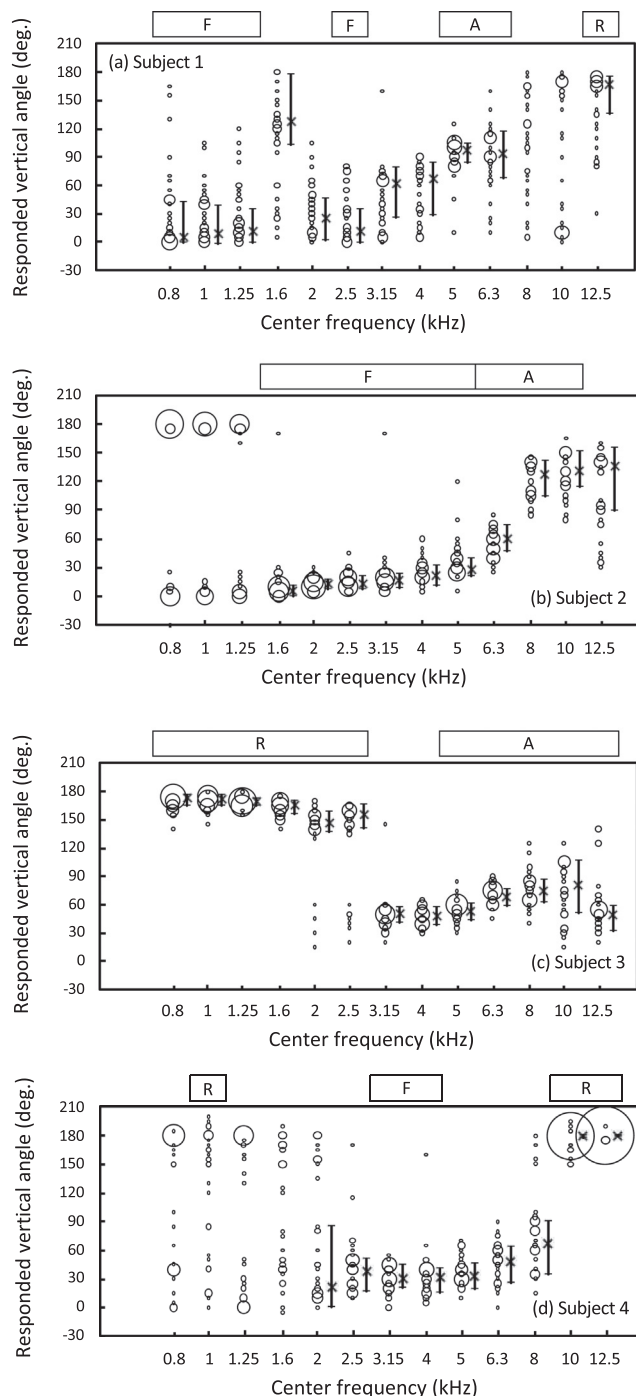


FIG. 3. Responded vertical angles (circles), ranges of responded vertical angles that could be considered to be directional bands (vertical bars), and their median values ("×"). The radius of each circle is proportional to the relative number of responses. For reference, the directional bands (front, above, and rear) analyzed by Itoh *et al.* (2007) are shown at the top of each panel.

same directions in the present analysis. Furthermore, even at frequencies that were not considered directional bands in the analysis by Itoh *et al.*—for example, 3.15 and 4 kHz—directional bands were observed in directions between the front and above.

For subject 2, the responded vertical angles were distributed separately around 0° and 180° at center frequencies between 0.8 and 1.25 kHz. In the analysis by Itoh *et al.*,

these three bands were not identified as the front, above, or rear directional bands. For frequencies above 1.6 kHz, as the center frequency of the stimulus increased to 12.5 kHz, the responded vertical angles increased from 1° to 163°, with a few exceptions. Directional bands were observed at all center frequencies above 1.6 kHz, and the median vertical angles that could be considered to be directional bands increased from 6° to 136° as the frequency increased.

The directional bands analyzed by Itoh *et al.* were 1.6–5 kHz for the front and 6.3–10 kHz for the above direction. In the present analysis, the directional band shifted continuously from front to above over this frequency range.

For subject 3, the responded vertical angles were distributed between 140° and 180° at center frequencies from 0.8 to 2.5 kHz. For frequencies above 3.15 kHz, the response vertical angles increased from 21° to 139° as the center frequency increased up to 12.5 kHz. Directional bands were observed at all center frequencies. The median vertical angles that could be considered to be directional bands ranged from 146° to 173° for 0.8–2.5 kHz, 50° to 81° for 3.15–10 kHz, and 50° for 12.5 kHz.

The directional bands analyzed by Itoh *et al.* were 0.8–2.5 kHz for the rear and 5–12.5 kHz for the above direction. At these frequencies, directional bands were observed in similar directions in the present analysis. However, from 5 to 10 kHz, the median responded vertical angles shifted continuously from 54° to 81°.

For subject 4, the responded vertical angles were distributed over a wide range from −1° to 199° at center frequencies between 0.8 and 2 kHz. From 2.5 to 8 kHz, the response vertical angles increased from 9° to 100° with increasing center frequency, except for a few outliers. At 10 and 12.5 kHz, the responses ranged from 148° to 195°. Directional bands were observed from 2 to 12.5 kHz. The median vertical angles that could be considered to be directional bands increased from 22° to 67° as the center frequency increased from 2 to 8 kHz. At 10 and 12.5 kHz, the median was 180°.

The directional bands analyzed by Itoh *et al.* were 1 kHz for the rear, 3.15 and 4 kHz for the front, and 10 and 12.5 kHz for the above direction. At these frequencies—except for 1 kHz—directional bands were observed in similar directions in the present analysis.

To summarize, from 0.8 to 2.5 kHz, directional bands were observed in either the rear or front direction. From 3.15 to 8 kHz, the directional band shifted continuously from the front toward the above direction as the center frequency increased. At 10 and 12.5 kHz, directional bands were observed between the above and rear directions.

These results indicate that directional bands were not limited to the front, above, or rear directions, but instead were distributed continuously across the entire upper median plane.

B. Comparison between perceived vertical angle and dominant vertical angle for each directional band

Having shown that directional bands exist continuously throughout the upper median plane, we next consider what

determines their perceived median vertical angles. As a first step, we investigate whether these angles correspond to the direction in which the HRTF energy is maximal for a given frequency band.

Blauert (1969/70) analyzed HRTFs and reported that, in the directional band for the front direction, the HRTF energy was greater for the front than for the rear direction. Referring to this, we calculated the energy of each 1/3-octave-band with center frequencies ranging from 0.8 to 12.5 kHz, using the subject's own HRTFs measured at seven vertical angles (0° to 180° , in 30° intervals) in the upper median plane. The analysis was conducted for the subjects whose directional bands were identified in Sec. IV A.

For each 1/3-octave-band for the left and right ears, the vertical angle at which the energy was highest across all tested vertical angles was identified. This vertical angle is hereafter referred to as the dominant vertical angle.

Figure 4 shows the dominant vertical angles plotted alongside the data presented in Fig. 3. The blue open squares represent the dominant vertical angles for the left ear, and the red filled circles represent those for the right ear. It should be noted that the responded vertical angles are continuous values, whereas the dominant vertical angles are limited to discrete values at 30° intervals.

For subject 1, as described above, directional bands were observed across the entire frequency range from 0.8 to 12.5 kHz, except 8 and 10 kHz. From 0.8 to 8 kHz, the dominant vertical angles generally coincided with the median vertical angles that could be considered to be directional bands. However, at 1 and 1.25 kHz, the dominant vertical angles for the left and right ears differed; those for the left ear approximately coincided with the median vertical angles that could be considered to be directional bands. At 1.6 kHz, the dominant vertical angle was 0° , whereas the corresponding median vertical angle that could be considered to be a directional band was 128° . At 12.5 kHz, the dominant vertical angle was 30° for the left ear and 60° for the right ear, whereas the median vertical angle that could be considered to be a directional band was 168° .

For subject 2, directional bands were observed from 1.6 to 12.5 kHz. From 1.6 to 8 kHz, the dominant vertical angles generally coincided with the median vertical angles that could be considered to be directional bands. At 10 and 12.5 kHz, however, the dominant vertical angles were 30° and 0° , respectively, whereas the corresponding median vertical angles that could be considered to be directional bands were 132° and 136° .

For subject 3, directional bands were observed across the entire frequency range from 0.8 to 12.5 kHz. From 0.8 to 1.25 kHz, the dominant vertical angles coincided with the median vertical angles that could be considered to be directional bands. However, from 1.6 to 2.5 kHz, the dominant vertical angles were 30° , 0° , and 0° , whereas the corresponding median vertical angles that could be considered to be directional bands were 166° , 146° , and 156° , respectively. While the dominant vertical angles in these three frequency bands were similar to those observed in the other

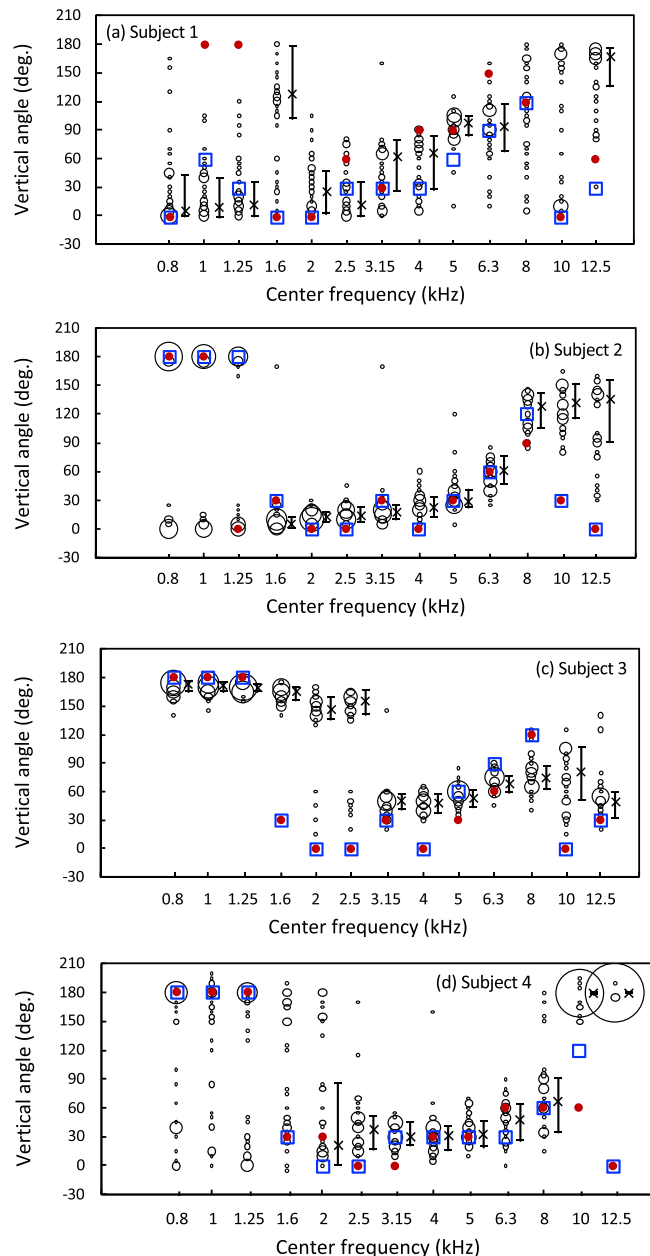


FIG. 4. Responded vertical angles (open circles), ranges of responded vertical angles that could be considered to be directional bands (vertical bars), their median values ("x"), and the dominant vertical angles (squares and circles). Blue open squares represent the dominant vertical angles for the left ear, and red filled circles represent those for the right ear. Note that the responded vertical angles are continuous values, whereas the dominant vertical angles are restricted to discrete values at 30° intervals.

subjects, the median vertical angles that could be considered to be directional bands were markedly different. The reason for this discrepancy remains unclear. At 3.15, 5, 6.3, and 12.5 kHz, the dominant vertical angles approximately coincided with the corresponding median vertical angles that could be considered to be directional bands. However, at 4 kHz, the dominant vertical angle was 0° , whereas the median vertical angle that could be considered to be a directional band was 48° . At 8 and 10 kHz, the dominant vertical angles were 120° and 0° , respectively, whereas the median

vertical angles that could be considered to be directional bands were 75° and 81°, respectively.

For subject 4, directional bands were observed from 2 to 12.5 kHz. From 2 to 8 kHz, the dominant vertical angles generally coincided with the median vertical angles that could be considered to be directional bands. At 10 kHz, the dominant vertical angles were 120° for the left ear and 60° for the right ear, and at 12.5 kHz, they were 0°; however, the corresponding median vertical angles that could be considered to be directional bands were 180° for both frequencies.

To summarize, the dominant vertical angles generally coincided with the median vertical angles that could be considered to be directional bands for center frequencies from 0.8 to 8 kHz. In other words, for this frequency range, the 1/3-octave-band in which the energy of the HRTF was highest at a certain vertical angle coincided with the 1/3-octave-band in which the sound image was perceived at that vertical angle—that is, the directional band.

On the other hand, for center frequencies of 10 and 12.5 kHz, the dominant vertical angles did not coincide with the median vertical angles that could be considered to be directional bands.

C. Dominant frequencies for seven vertical angles in the upper median plane

In Secs. IV A and IV B, we discussed directional bands and dominant vertical angles using 1/3-octave-bands. In this section, we analyze dominant frequencies across the upper median plane using discrete frequencies at 93.75 Hz resolution, based on HRTFs measured for seven vertical angles (0° to 180°, in 30° steps).

For a given ear, the dominant frequency for a specific vertical angle is defined as the frequency at which the sound pressure level of the HRTF is higher than that for any other vertical angle. Figure 5 shows the relationship between the dominant frequency and the vertical angle for 118 ears of 59 subjects. The radius of each circle is proportional to the relative number of ears. While there is some variability across subjects (see Sec. VIB), dominant frequencies are frequently observed at 0° and 30°, and less frequently at 120° and 150°.

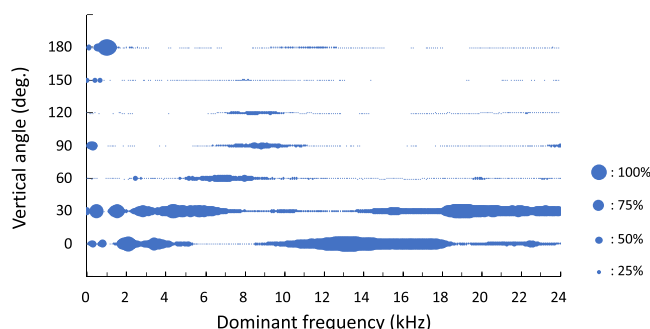


FIG. 5. Relationship between the dominant frequency and the vertical angle for 118 ears of 59 subjects. The radius of each circle is proportional to the relative number of ears.

These dominant frequencies tend to form clusters at specific frequency ranges for each vertical angle. Focusing on the 0.3–14.0 kHz range, which covers Blauert’s directional bands (see Table IV), we identified the following dominant frequency regions—defined as frequency regions with a high density of dominant frequencies.

At 0°, dominant frequency regions appear at approximately 0.3, 0.8, 1.7–2.5, 2.9–4.3, 4.7–5.1, and 8.5–14.0 kHz. The 2.9–4.3 kHz region corresponds to the P1 frequency (Table III). At 30°, multiple dominant frequency regions are observed at 0.5, 1.2–1.7, 2.3–3.3, and 3.5–7.3 kHz. At 60°, the dominant frequency region is 5.2–8.3 kHz. At 90°, two dominant frequency regions appear at approximately 0.3 kHz and 6.6–11.0 kHz. The 6.6–11.0 kHz region coincides with the P2 frequency. At 120°, the dominant frequency region is 7.3–10.6 kHz. At 150° and 180°, dominant frequency regions are observed below 2 kHz—specifically, 0.4–0.7 kHz for 150°, and 0.6–1.3 kHz for 180°, the latter aligning with the P0 frequency. Because HRTF components below 2 kHz are known to contribute to front-back localization (Asano *et al.*, 1990), these low-frequency dominant regions are presumed to play an important role in the perception of sound sources at 150° and 180°.

To simplify the analysis and ensure consistent terminology, we define a single dominant band for each vertical angle. A dominant band refers to the dominant frequency region most relevant to sound localization for a given vertical angle. For 60° and 120–180°, only one dominant frequency region is observed per angle, so the dominant band is identical to that region. For 0°, 30°, and 90°, multiple dominant frequency regions exist. In these cases, the dominant band is selected based on theoretical and perceptual relevance. For 0°, the 2.9–4.3 kHz region (aligned with P1) is selected; for 90°, the 6.6–11.0 kHz region (aligned with P2) is selected. For 30°, the 3.5–7.3 kHz region is selected as it lies near the straight line connecting P1 (the dominant band for 0°) and P2 (the dominant band for 90°).

The frequency ranges of the dominant bands are listed in Table V. The dominant bands are observed throughout the upper median plane, and they systematically shift with vertical angle: from around 3 kHz at 0°, increasing to approximately 11 kHz at 120°, then shifting to below 1 kHz at 150° and 180°.

D. Comparison of peak frequencies, directional bands, and dominant bands

We next compare the peak frequencies, directional bands, and dominant bands for the seven vertical angles in the upper median plane.

TABLE V. Frequency ranges of dominant bands in the upper median plane (kHz).

Vertical angle in the upper median plane (deg.)						
0	30	60	90	120	150	180
2.9–4.3	3.5–7.3	5.2–8.3	6.6–11.0	7.3–10.6	0.4–0.7	0.6–1.3

First, we focus on 0° , 90° , and 180° . As shown in Tables III and IV, the directional bands for these angles coincide with the P1, P2, and P0 frequencies, respectively—frequencies that contribute to the perception of 0° , 90° , and 180° . In addition, as described in Sec. IV C (see Fig. 5, Table V), the dominant bands for these angles also coincide with the corresponding peak frequencies. In other words, for 0° , 90° , and 180° , the P1, P2, and P0 frequencies, directional bands, and dominant bands are all aligned. This suggests that the dominant bands in the HRTFs for these directions serve as cues for vertical angle perception.

Next, we consider the other vertical angles in the upper median plane. No previous studies have identified specific spectral peaks analogous to P1, P2, or P0 for angles other than 0° , 90° , and 180° . However, as shown in Sec. IV B (Fig. 4), from 0.8 to 8 kHz, the dominant vertical angle—defined as the vertical angle with the maximum HRTF energy for a given 1/3-octave-band—generally coincides with the median vertical angle that could be considered to be a directional band. That is, from 0.8 to 8 kHz, the 1/3-octave-band in which the HRTF energy is maximal for a given vertical angle (a dominant band) tends to match the band in which the sound image is perceived at that angle (a directional band). However, for frequencies below 0.8 kHz, this correspondence has not been directly confirmed and in some cases may not be established, and for center frequencies of 10 and 12.5 kHz, the dominant and directional bands do not coincide (as shown in Fig. 4). These observations imply that the dominant bands in the range of 0.8–8 kHz in the HRTFs for these vertical angles also serve as cues for vertical angle perception, in the same way as for 0° , 90° , and 180° .

Taken together, these findings suggest that the dominant bands in the range of 0.8–8 kHz in the HRTF for each vertical angle in the upper median plane act as a cue for the perception of vertical angle.

E. Mean dominant level for the dominant frequency for seven vertical angles in the upper median plane

The mean dominant level (MDL) for the dominant frequency was next calculated to assess how distinctly the dominant frequency stands out across different vertical angles. Using the HRTFs of each pinna for the seven vertical angles in the upper median plane, we calculated the average difference between the maximum amplitude level of the seven directions and the amplitude levels of the other six directions for each discrete frequency. Then, we calculated the mean value averaged over 118 ears for each discrete frequency using Eq. (1),

$$MDL(f) = \frac{1}{118} \sum_{i=1}^{118} \left[\frac{1}{6} \sum_{j=1}^7 \{L(i,f)_{\max} - L(i,j,f)\} \right] \quad (1)$$

for $L(i,f)_{\max} \neq L(i,j,f)$,

where i is the ear number (1–118), j is the vertical angle number (1–7), f is the discrete frequency, and L and L_{\max}

denote the amplitude level and the maximum amplitude level of the HRTF, respectively.

The MDL and the 95% confidence interval are shown in Fig. 6. The MDL tends to increase with increasing frequency. In the 0.3–14 kHz range, which covers the Blauert (1969/70) directional bands (see Table IV), the MDL is approximately 3–13 dB, except around 0.3 kHz. This range exceeds the detection threshold of a spectral peak (Moore *et al.*, 1989). The 95% confidence interval is less than 0.7 dB. It is well-known that there are large individual differences in the amplitude spectrum of HRTF (Iida, 2019a), but compared to this, the individual differences in the MDL are small.

F. Reason why P1 is necessary throughout the upper median plane

In Sec. IV D, we showed that the P1 frequency coincides with both the directional band and the dominant band for the front direction. From the perspective of the directional band theory, this alignment suggests that P1 plays a key role in front localization by providing a salient spectral peak that serves as the dominant band for this direction. However, as shown in Table I, previous studies have reported that P1 is required not only for the front direction but also throughout the upper median plane (Iida *et al.*, 2007). A possible reason for this is provided in the following.

Introspection reports of conventional sound localization tests using headphones (Iida *et al.*, 2007; Iida and Ishii, 2018) have pointed out that excluding P1 from the PNP model often results in inside-of-head localization. In addition, P1 has been identified as a resonance of the concha cavity, with a consistently high amplitude around 3–4 kHz regardless of the direction of incidence (Teranishi and Shaw, 1968). In other words, P1 represents a spectral peak that characterizes sound waves arriving from outside the head, being affected by the pinnae, and reaching the eardrum. Therefore, in addition to contributing to the perception of the front direction, P1 is thought to contribute to out-of-head localization regardless of the vertical angle of the sound source. This is thought to be the reason why P1 is required throughout the upper median plane.

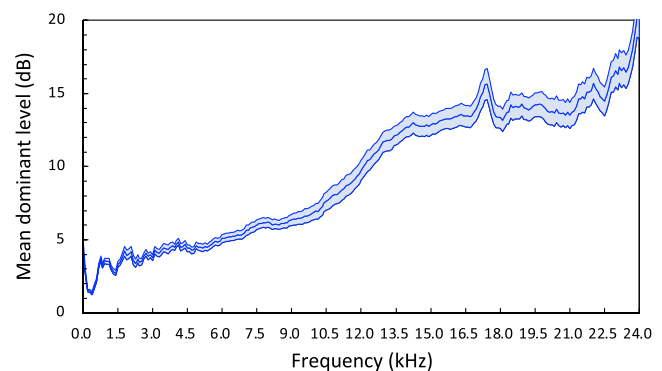


FIG. 6. Mean dominant level and 95% confidence interval across the seven vertical angles in the upper median plane, averaged across 118 ears.

G. Hypothesis 2: Cues for vertical angle perception in the upper median plane

From these findings, it can be inferred that dominant bands in the range of 0.8–8 kHz act as cues for vertical angle perception in the upper median plane. Based on this inference, we propose Hypothesis 2 as follows: The dominant bands—those in the range of 0.8–8 kHz—whose frequency coincides with that of the directional bands, together with N1 and N2, act as cues for vertical localization in the upper median plane. In addition, P1, the frequency of which does not depend on the vertical angle of the sound source, contributes to out-of-head localization.

V. EXTENSION OF PARAMETRIC NOTCH-PEAK HRTF MODEL

Based on Hypothesis 2 discussed in Sec. IV, we extended the PNP model to account for vertical angle perception in the upper median plane. In the extended PNP model, the dominant peak (Pd), which reflects the dominant band, replaces P2 and P0 in the conventional model. The frequency of the Pd is defined as the center frequency of the corresponding dominant band. The resulting model consists of N1, N2, P1, and Pd. At 0°, 90°, and 180°, the model configuration remains unchanged, but for other vertical angles, Pd is added as a direction-specific peak.

Figure 7 shows N1, N2, P1, and Pd for a representative subject. N1, N2, and P1 are indicated by solid lines, and Pd by dashed lines. White filled circles denote Pd for 0°, 90°, and 180°, which coincide with the frequencies of P1, P2, and P0 in the conventional model. Black filled circles denote Pd for 30°, 60°, 120°, and 150°.

The Pd for 0° to 120° increases monotonically from approximately 4 to 8 kHz. The Pds for 30°, 60°, and 120° align with the straight line connecting the P1 frequency for 0° and the P2 frequency for 90°. This line traverses arc-shaped regions of high sound pressure (shown in red), lies nearly parallel to the N1 trajectory, and is approximately 2 kHz lower than the N1. On the other hand, the Pds for 150° and 180° are located in a separate diagonal stripe-like region spanning 0.5 to 1 kHz. Thus, the Pd shows a

discontinuity between 120° and 150°, extracted from the subject's HRTFs using the method described in Sec. IV C.

For the HRTFs generated by the conventional PNP model, the variance in perceived vertical angle was greater for target vertical angles of 60° and 120° than for 0°, 90°, and 180° (Nakamura *et al.*, 2024). The extended PNP model is expected to improve localization accuracy for target vertical angles with ambiguous sound images by reproducing Pd.

Furthermore, enhancing Pd in the extended PNP model may enable the generation of HRTFs that surpass the localization accuracy of a subject's own measured HRTFs, particularly under noisy conditions. In everyday situations, we often perceive the direction of a target sound in the presence of environmental noise, which has been reported to degrade localization accuracy (Good and Gilkey, 1996). This degradation is more pronounced in the vertical direction than in the lateral direction. One reason for this is that interaural time and level differences—important cues for lateral localization—are often preserved even in noisy conditions, whereas spectral notches used for vertical localization can become undetectable due to noise. In addition, the sensation level of spectral peaks may be reduced by masking. Since notches remain buried in noise even if they are deepened, little improvement in vertical localization accuracy is expected. In contrast, increasing the level of Pd may improve vertical localization by making direction-specific spectral cues more salient.

VI. DISCUSSION

This section addresses the following five issues: (1) interpretation of previous experimental results in light of Hypothesis 2, (2) individual differences in dominant bands, (3) possible anatomical origins of dominant bands, (4) learning of dominant bands, and (5) learning of directional bands.

A. Interpretation of previous experimental results based on Hypothesis 2

Using Hypothesis 2 proposed in Sec. IV, we interpret the results of the sound image localization tests for narrow-band and wideband signals introduced in Sec. II B.

First, we attempt to explain the results of the sound image localization tests using narrow-band signals. In the tests, in which Blauert (1969/70) found the directional bands, the stimuli were 1/3-octave-band noise, so the subject's ear-input signals contained only components that were convolved with the 1/3-octave-band noise and the HRTFs for either the front, above, or rear direction. The reason why the sound image was not perceived in the direction of the loudspeaker that presented the stimuli is thought to be because the ear-input signals lacked N1, N2, P1, and Pd corresponding to the vertical angle of the loudspeaker, except in cases where 1/3-octave-band noise corresponding to P1, which is also Pd for the front direction, was presented from the front loudspeaker, or where 1/3-octave-band noise

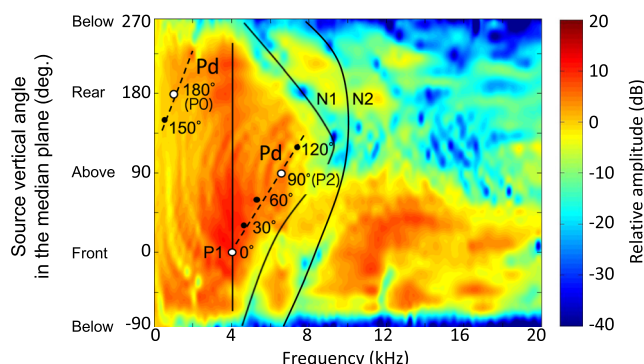


FIG. 7. Relationships between N1, N2, and P1 (solid lines), and Pd (dashed lines) for a representative subject in the median plane. Black filled circles denote Pds for 30°, 60°, 120°, and 150°, whereas white filled circles denote those for 0°, 90°, and 180°.

corresponding to Pd for the above, or rear directions was presented from the respective loudspeakers.

Next, we attempt to explain the results of sound localization tests using wideband white noise stimuli with a certain 1/3-octave-band boosted. In this case, the ear-input signals included N1, N2, Pd, and P1 corresponding to the loudspeaker's vertical angle. Although the boosted 1/3-octave-band coincided with a directional band for either the front, above, or rear direction, N1 and N2 for that directional band were absent in the signal. As such, the directional band alone is not considered sufficient for vertical localization of wideband signals. This is thought to be the reason why the sound image was perceived in the direction of the loudspeaker rather than in the direction associated with the boosted directional band.

B. Individual differences in dominant bands

We next examine individual differences in the dominant bands. Figure 8 shows the dominant frequencies for three representative ears, selected from 118 ears, as described in Sec. IV C (see Fig. 5). As shown in Table V, the dominant band for each vertical angle lies approximately within the following frequency ranges: 2.9–4.3 kHz for 0°, 3.5–7.3 kHz for 30°, 5.2–8.3 kHz for 60°, 6.6–11.0 kHz for 90°, 7.3–10.6 kHz for 120°, 0.4–0.7 kHz for 150°, and 0.6–1.3 kHz for 180°. Based on these ranges, the dominant band for each ear in Fig. 8 was extracted from its respective dominant frequencies.

For Ear 1, the center frequency of the dominant band for vertical angles from 0° to 120° increased from 3.6 to 9.9 kHz. For 150° and 180°, the dominant bands were around 0.4 and 0.9 kHz, respectively. For Ear 2, the corresponding values were 3.9 to 9.0 kHz for 0° to 120°, and around 0.4 and 0.9 kHz for 150° and 180°. For Ear 3, the dominant band increased from 3.2 to 6.8 kHz across 0° to 120°, and was located around 0.5 and 0.9 kHz for 150° and 180°.

These results indicate that while the dominant band shifts upward in frequency with increasing vertical angle from 0° to 120° in a similar pattern across ears, the exact frequency values vary. In contrast, the dominant frequencies at 150° and 180° show much smaller inter-individual variation.

One possible explanation for this inter-individual variation relates to the frequency range of the dominant bands. For 0° to 120°, the dominant bands lie above 4 kHz, a region known to exhibit large inter-individual differences in HRTF spectra (Iida, 2019a). From a wavelength perspective, this variability is presumed to be attributable to differences in pinna shape.

On the other hand, the dominant band for 180° lies near 1 kHz, where the effect of the pinnae is minimal. Shaw (1997) reported that in the frontal sector of the horizontal plane, a spectral notch occurs from around 1 to 1.3 kHz due to interference between direct sound and reflections from the shoulders. This phenomenon does not appear in rear HRTFs, and the 1–1.3 kHz band lies somewhat above the

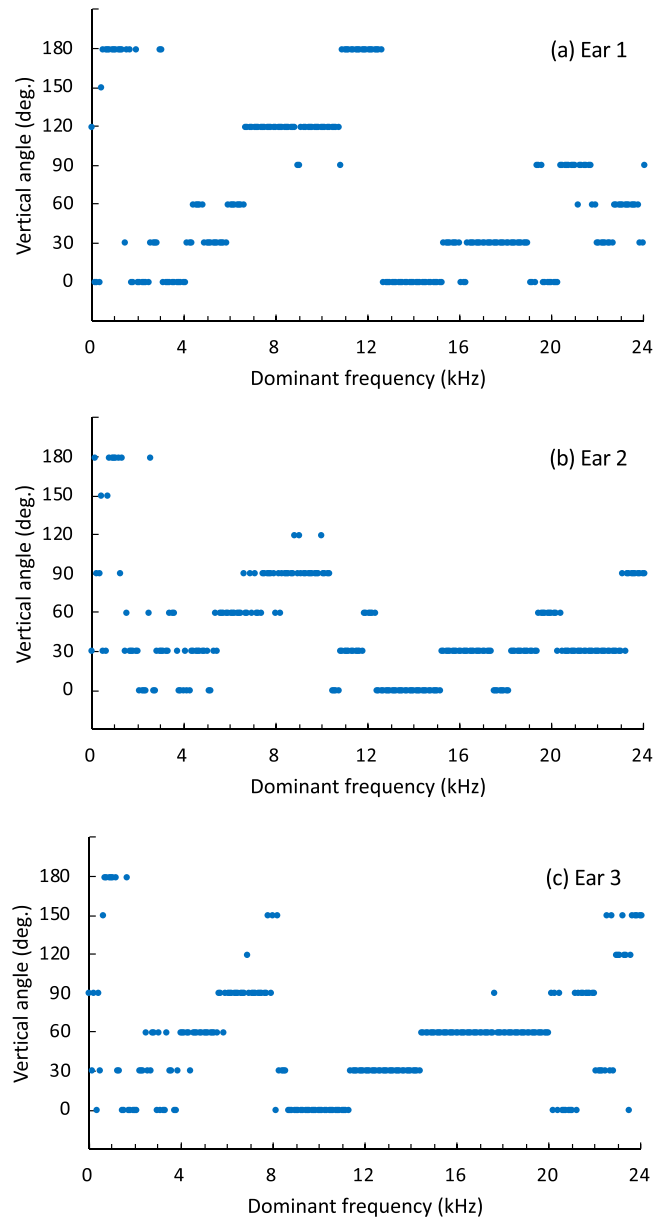


FIG. 8. Relationship between the dominant frequency and vertical angle for three representative individual ears.

lower edge of the concha resonance centered at 3–4 kHz, often exhibiting a relatively high sound pressure level. The dominant band for 180° is presumed to be shaped by these two acoustic effects. Compared to the large variability in pinna shape, individual differences in the geometry of the shoulders and torso are relatively small, which may explain the limited variation in the 180° dominant band.

C. Possible anatomical origins of dominant bands

The dominant bands observed across the upper median plane are shaped by the acoustic filtering effects of the external ear and surrounding structures. While the present study did not directly measure the physical origins of each dominant band, relevant insights can be drawn from previous anatomical and acoustic analyses of HRTFs. In the following, we consider

possible generation mechanisms separately for vertical angles from 0° to 120° and for those at 150° and 180°.

For vertical angles from 0° to 120°, the dominant bands appear to arise primarily from the combined effects of the P1 and P2 resonances. Previous studies have reported that P1 is the first resonance mode generated in the depth direction of the concha, with a frequency corresponding to the inverse of the wavelength equal to four times the concha cavity depth (Takemoto *et al.*, 2012). P1 is observed regardless of the vertical angle of incidence, as described in Sec. IV F, because the depth direction of the concha is approximately orthogonal to all vertical angles along the median plane; however, it is most prominent for the front (0°) direction. One possible reason is the protrusion of the pinna (Burkhard and Sachs, 1975), which orients the aural axis slightly toward the front, so sound arriving from near-frontal directions may more efficiently excite the concha-cavity resonance. The origin of P2 has been attributed to the first resonance mode in the vertical direction of the pinna cavities, generated along the pinna surface, with two phase-reversed antinodes located near the entrance of the ear canal and the upper part of the pinna cavities (Takemoto *et al.*, 2012). It is therefore inferred that P1 is most prominent at a vertical angle of 0° and P2 at 90°, whereas at other vertical angles, a peak may arise from a weighted combination of P1 and P2. This interpretation is consistent with the observation that the dominant bands for angles between 0° and 120° change continuously with vertical angle, suggesting that intermediate directions may not correspond to unique anatomical sites, but rather to varying contributions from these two primary resonance modes.

For vertical angles of 150° and 180°, the acoustic mechanisms shaping the dominant bands are discussed in Sec. VIB (“Individual differences in dominant bands”). Briefly, the dominant band near 1 kHz is situated where the effect of the pinnae is minimal, and is presumed to be shaped by a combination of shoulder-reflection effects and the lower edge of the concha resonance. These factors result in relatively small inter-individual variation in the 180° dominant band compared to other directions.

While speculative, this interpretation is consistent with prior anatomical and acoustic findings and provides a coherent framework for understanding the continuous variation of dominant bands. It may also serve as a working hypothesis for future experimental studies.

D. Learning of dominant bands

We discuss the learning of dominant bands. It can be considered that when we listen to sound, we may not learn the spectrum of the HRTF for each vertical angle of a sound source individually, but rather, acquire the spectral features of the HRTFs by comparing them across different vertical angles. This suggests that we may acquire knowledge of which frequency is dominant for a certain vertical angle, or conversely, which vertical angle is dominant for a certain frequency, and use this knowledge as one of the cues for vertical angle perception.

E. Learning of directional bands

Finally, we discuss learning of directional bands. It is implausible to assume that we learn directional bands by listening to narrow-band signals, such as 1/3-octave-bands, in our daily lives. Rather, it is more plausible that we learn dominant bands through everyday experience with wide-band sounds. As a result, we may perceive a sound image at a specific vertical angle for the directional band, whose frequency range matches the dominant band.

VII. CONCLUSIONS

In the present study, we first focused on the three principal directions (front, above, and rear) in the median plane and discussed the results of previous research on the PNP HRTF model and the directional band theory together with recent analytical results, with the aim of integrating these two findings. We then expanded the scope of the sound source direction to the entire upper median plane and proposed a hypothesis regarding the cues for the perception of vertical angle. Furthermore, we extended the PNP model based on this hypothesis. The conclusions are as follows:

- (1) Integration of previous findings from both the directional band theory and the original PNP model, combined with the analytical results obtained in the present study, indicates that the original PNP model comprises notches and peaks, with peak frequencies corresponding to those of the directional bands for the front, above, and rear directions.
- (2) It is inferred that dominant bands in the range of 0.8–8 kHz—whose frequency coincides with that of the directional bands—together with N1 and N2, act as cues for vertical localization in the upper median plane, whereas P1, whose frequency does not depend on the vertical angle of the sound source, contributes to perception for the front direction and out-of-head localization.
- (3) An extended PNP model is proposed that consists of N1, N2, P1, and the dominant Peak (Pd), which reflects the dominant band. This extended model provides a more comprehensive HRTF model, using the minimum configuration of the spectral cues for vertical angle perception in the upper median plane.

ACKNOWLEDGMENTS

This research was supported in part by JSPS KAKENHI Grant No. 24K15052. We would also like to thank Dr. Masayuki Morimoto, Professor Emeritus of Kobe University, and Dr. Motokuni Itoh of Panasonic Corporation for informative discussions.

AUTHOR DECLARATIONS

Conflict of Interest

The authors have no conflicts to disclose.

Ethics Approval

The present paper does not include experiments using animal subjects and/or human participants.

DATA AVAILABILITY

The data that support the findings of this study are available within the article.

- Asano, F., Suzuki, Y., and Sone, T. (1990). "Role of spectral cues in median plane localization," *J. Acoust. Soc. Am.* **88**, 159–168.
- Blauert, J. (1969/70). "Sound localization in the median plane," *Acustica* **70**, 205–213.
- Burkhard, M. D., and Sachs, R. M. (1975). "Anthropometric manikin for acoustic research," *J. Acoust. Soc. Am.* **58**, 214–222.
- Butler, A., and Belendiuk, K. (1977). "Spectral cues utilized in the localization of sound in the median sagittal plane," *J. Acoust. Soc. Am.* **61**, 1264–1269.
- Good, M. D., and Gilkey, R. H. (1996). "Sound localization in noise: The effect of signal-to-noise ratio," *J. Acoust. Soc. Am.* **99**, 1108–1117.
- Hebrank, J., and Wright, D. (1974). "Spectral cues used in the localization of sound sources on the median plane," *J. Acoust. Soc. Am.* **56**, 1829–1834.
- Iida, K. (2019a). *Head-Related Transfer Function and Acoustic Virtual Reality* (Springer Nature, Singapore), Chap. 4.
- Iida, K. (2019b). *Head-Related Transfer Function and Acoustic Virtual Reality* (Springer Nature, Singapore), Chap. 6.
- Iida, K., and Ishii, Y. (2018). "Effects of adding a spectral peak generated by the second pinna resonance to a parametric model of head-related transfer functions on upper median plane sound localization," *Appl. Acoust.* **129**, 239–247.
- Iida, K., Itoh, M., Itagali, A., and Morimoto, M. (2007). "Median plane localization using parametric model of the head-related transfer function based on spectral cues," *Appl. Acoust.* **68**, 835–850.
- Itoh, M., Iida, K., and Morimoto, M. (2007). "Individual differences in directional bands," *Appl. Acoust.* **68**, 909–915.
- Mehrgardt, S., and Mellert, V. (1977). "Transformation characteristics of the external human ear," *J. Acoust. Soc. Am.* **61**, 1567–1576.
- Møller, H. (1992). "Fundamentals of binaural technology," *Appl. Acoust.* **36**, 171–218.
- Moore, B. C. J., Oldfield, R., and Dooley, G. J. (1989). "Detection and discrimination of peaks and notches at 1 and 8 kHz," *J. Acoust. Soc. Am.* **85**, 820–836.
- Musicant, A., and Butler, R. (1984). "The influence of pinnae-based spectral cues on sound localization," *J. Acoust. Soc. Am.* **75**, 1195–1200.
- Nakamura, F., and Iida, K. (2025). "Cue for rear sound image localization in head-related transfer function below 4 kHz," *Appl. Acoust.* **229**, 110370.
- Nakamura, F., Kako, T., Watanabe, Y., Chiba, H., Noguchi, K., and Iida, K. (2024). "Optimization of notch and peak levels of PNP HRTF model—Verification of sound image localization accuracy using two kinds of headphones," *Proc. Annu. Autumn Mtgs. Acoust. Soc. Jpn.* **2024**, 385–388 (in Japanese).
- Rayleigh, Lord (1877). "Acoustical observations," *Philos. Mag.* **3**, 456–464.
- Rayleigh, Lord (1907). "On our perception of sound direction," *Philos. Mag.* **13**, 214–232.
- Sayers, B. M. (1964). "Acoustic-image localization judgements with binaural tones," *J. Acoust. Soc. Am.* **36**, 923–926.
- Shaw, E. A. G. (1997). *Binaural and Spatial Hearing Real and Virtual Environments* (Lawrence Erlbaum Associates, Mahwah, NJ), Chap. 2.
- Shaw, E. A. G., and Teranishi, R. (1968). "Sound pressure generated in an external-ear replica and real human ears by a nearby point source," *J. Acoust. Soc. Am.* **44**, 240–249.
- Takemoto, H., Mokhtari, P., Kato, H., Nishimura, R., and Iida, K. (2012). "Mechanism for generating peaks and notches of head-related transfer functions in the median plane," *J. Acoust. Soc. Am.* **132**, 3832–3841.
- Teranishi, R., and Shaw, E. A. G. (1968). "External-ear acoustic models with simple geometry," *J. Acoust. Soc. Am.* **44**, 257–263.
- Toole, F. E., and Sayers, B. M. (1965). "Lateralization Judgements and the Nature of Binaural Acoustic Images," *J. Acoust. Soc. Am.* **37**, 319–324.